

# Numerical Study of Induced False Vacuum Decay at High Energies

A.N.Kuznetsov and P.G.Tinyakov

*Institute for Nuclear Research of the Russian Academy of Sciences,  
60th October Anniversary prospect, 7a, Moscow 117312, Russia.*

October 1995

## Abstract

We calculate numerically the probability  $\exp[\frac{1}{\lambda}F(E/E_{sph}, N/N_{sph})]$  of the false vacuum decay in the massive four-dimensional  $-\lambda\phi^4$  model from multiparticle initial states with fixed number of particles  $N$  and energy  $E$  greater than the height of the barrier  $E_{sph}$ . We find that at  $E \lesssim 3E_{sph}$  and  $N \lesssim 0.4N_{sph}$  the decay is classically forbidden and thus is exponentially suppressed. We argue that the classically forbidden region extends at small  $N$  at least up to  $E \sim 10E_{sph}$  and, most likely, to all energies. Our data suggest that the false vacuum decay induced by two-particle collisions is exponentially suppressed at all energies.

# 1 Introduction

In the last few years a substantial progress has been made in understanding of non-vacuum tunneling in field theory. The interest to this subject is inspired by attempts to calculate, in the Standard Model, the instanton-mediated baryon number violation in particle collisions at high energy [1]. Although a variety of methods has been developed for calculating the tunneling probabilities at  $E \ll E_{sph}$ , where  $E_{sph}$  is the height of the barrier (the sphaleron energy in the Electroweak Theory), the behaviour of probabilities in the most interesting region  $E \gtrsim E_{sph}$  is still unknown (for a review see ref.[2]). In particular, the question of whether the exponential suppression of baryon number violating processes disappears at some sufficiently high energy of colliding particles, still remains unanswered. Since analytical approaches to tunneling induced by particle collisions seem to be exhausted, in the present paper we address this problem by means of numerical methods.

A suitable starting point for numerical study of non-vacuum tunneling is provided by the semiclassical approach developed in refs.[3, 4, 5]. In this approach the key role is played by the probability of tunneling from a mixed state with fixed energy  $E$  and number of particles  $N$ . This probability is defined as follows,

$$\sigma(E, N) = \sum_{i,f} |\langle f | \hat{S} \hat{P}_E \hat{P}_N | i \rangle|^2,$$

where  $\hat{S}$  is the S-matrix,  $\hat{P}_{E,N}$  are projectors onto subspaces of fixed energy  $E$  and fixed number of particles  $N$ , respectively, while the states  $|i\rangle$  and  $|f\rangle$  are perturbative excitations above two vacua lying on different sides of the barrier. It was argued in refs.[3, 4] that at any fixed  $N$ , the probability  $\sigma(E, N)$  sets an upper bound for the two-particle cross section, while in the limit of small  $N$  this probability reproduces the two-particle cross section with exponential accuracy.

The advantage of considering multiparticle probability  $\sigma(E, N)$  instead of two-particle one is that in the weak coupling regime  $g^2 \rightarrow 0$  and  $E, N \sim 1/g^2$ , the former can be calculated semiclassically and has the form

$$\sigma(E, N) \sim \exp\left\{\frac{1}{g^2} F(\epsilon, \nu)\right\}, \quad (1)$$

where  $\epsilon = E/E_{sph}$ ,  $\nu = N/N_{sph}$  and  $N_{sph} \sim 1/g^2$  is the number of particles produced in the sphaleron decay. The function  $F(\epsilon, \nu)$  is negative at low energies, which corresponds to exponential suppression of probability in this domain. At  $\epsilon = 1$  and  $\nu = 1$  (at the sphaleron), the function  $F(\epsilon, \nu)$  vanishes, i.e. the exponential suppression disappears. The absence of exponential suppression of the two-particle cross section would show up as zero of the function  $F(\epsilon, \nu)$  at some fixed  $\epsilon > 1$  and  $\nu \rightarrow 0$ .

The function  $F(\epsilon, \nu)$  is determined by a solution to the specific classical boundary value problem for the complexified field equations [5]. Namely, one has to solve the

usual field equation

$$\frac{\delta S}{\delta \phi} = 0, \quad (2)$$

where time and the field  $\phi$  are treated as complex variables. All the information about particular problem is encoded into the boundary conditions, which are formulated on the contour ABCD in the complex time plane (see Fig.1). The asymptotic regions A and D correspond to the initial and final states, respectively.

The boundary conditions are as follows. The final boundary condition states that the field is real on the line CD, where it represents the classical evolution of the system after barrier penetration. This requirement can be imposed at the point C where it implies

$$\begin{aligned} \text{Im } \phi &= 0, \\ \text{Im } \frac{\partial \phi}{\partial t} &= 0. \end{aligned} \quad (3)$$

The part CD of the contour is not essential for formulation of these boundary conditions. In fact, this part does not play any role in the calculation of the function  $F(\epsilon, \nu)$  and can be dropped, unless the details of the final state are of interest. Due to this fact the final boundary conditions (3) apply also to  $-\lambda\phi^4$  model where the stable vacuum does not exist and field develops a singularity in the final state, i.e. somewhere on the line CD (point P in Fig.1).

At the other end of the contour, in the asymptotic region A, the field is required to be linear. The initial boundary conditions fix the ratio of amplitudes in the negative- and positive-frequency parts to be a constant independent of momentum. If one writes general asymptotics of the field in the form

$$\phi(x) = \int \frac{d\mathbf{k}}{\sqrt{(2\pi)^3 2\omega_k}} \left\{ e^{-\theta} f_{\mathbf{k}} e^{-i\omega_k \eta + i\mathbf{k}\mathbf{x}} + g_{\mathbf{k}} e^{i\omega_k \eta - i\mathbf{k}\mathbf{x}} \right\}, \quad (4)$$

where  $\eta = \text{Re } t$  and  $\theta$  is a real positive parameter, then the boundary condition is

$$g_{\mathbf{k}} = (f_{\mathbf{k}})^*. \quad (5)$$

This equation fixes one particular linear combination of the field and its time derivative. In total, there are two real conditions at each end of the contour for the second order complex differential equation, so in general the boundary value problem is completely specified.

The input variables  $E$  and  $N$  enter the above boundary conditions through two parameters:  $\theta$ , which enters the boundary conditions explicitly, and  $T$ , which is the amount of Euclidean evolution (see Fig.1) and specifies the place where initial boundary conditions are imposed. The relation between  $T$ ,  $\theta$  and  $E$ ,  $N$  is given by the equations

$$E = -\frac{\partial}{\partial T} \text{Re}[iS(T, \theta)],$$

$$N = -2 \frac{\partial}{\partial \theta} \operatorname{Re}[iS(T, \theta)], \quad (6)$$

where  $S(T, \theta)$  is the action of the solution for given  $T$  and  $\theta$ , evaluated along the contour. Note that according to boundary conditions (3) the field is real on the line CD, so that this part of the contour does not contribute into  $\operatorname{Re}[iS(T, \theta)]$ . Alternatively, the energy and the number of particles can be read off from the initial asymptotics of the field,

$$\begin{aligned} N &= \int d\mathbf{k} f_{\mathbf{k}} f_{\mathbf{k}}^*, \\ E &= \int d\mathbf{k} \omega_{\mathbf{k}} f_{\mathbf{k}} f_{\mathbf{k}}^*. \end{aligned} \quad (7)$$

One can check that eqs.(6) and (7) coincide, provided that eqs.(2) and (5) are satisfied.

Given the solution to the boundary value problem one can calculate the function  $F(\epsilon, \nu)$  according to the formula

$$\frac{1}{g^2} F(\epsilon, \nu) = 2ET + N\theta + 2 \operatorname{Re}[iS(T, \theta)], \quad (8)$$

where  $T$  and  $\theta$  depend on  $E$  and  $N$  through eqs.(6).

Several remarks are in order. First, as follows from eqs.(4) and (5), at  $\theta \neq 0$  the solution is necessarily complex along the line AB. Thus, contributions to the function  $F(\epsilon, \nu)$  come from both Minkowskian (AB) and Euclidean (BC) parts of the contour. Second, as the field equations are analytic in time, the solution is also analytic everywhere except possible singularities. Thus, the contour ABC can be deformed, provided that the asymptotic region A is untouched and singularities are not crossed. In fact, one *must* expect singularities in between the contour ABC and the negative part of the real time axis. Otherwise the reality of the field at real  $t$  and the initial boundary conditions are incompatible. In the model we consider below these singularities lie on the real time axis, as shown in Fig.1. In numerical calculations it is convenient to deform the contour in such a way that it passes far from singularities (dotted line in Fig.1).

In one particular case, namely at  $\theta = 0$ , the above boundary value problem simplifies considerably. In this case the initial boundary conditions, eq.(5), reduce to the reality condition imposed at  $\operatorname{Im} t = T$ . The solution to the resulting boundary value problem is given by periodic instanton of ref.[6]. Periodic instanton is a real periodic solution to the Euclidean field equations with period  $2T$  and two turning points at  $t = 0$  and  $t = iT$ . Being analytically continued to the Minkowskian domain through the turning points, periodic instanton stays real at lines  $\operatorname{Im} t = 0$  and  $\operatorname{Im} t = T$  and thus satisfies the boundary conditions with  $\theta = 0$ .

The periodic instanton can be found analytically in two extreme cases: at  $\epsilon \ll 1$  it can be approximated by the periodic chain of instantons and antiinstantons, while at  $1 - \epsilon \ll 1$  it is approximately given by the oscillations in the sphaleron negative mode. At intermediate energies the periodic instanton can be obtained numerically [7, 8]. In

the  $\epsilon$ - $\nu$  plane, periodic instantons form a line connecting the points  $\epsilon = \nu = 0$  (zero energy instanton) and  $\epsilon = \nu = 1$  (sphaleron). The function  $F(\epsilon, \nu)$  monotonically grows from  $F(0, 0) = -S_{inst}$  to  $F(1, 1) = 0$  along this line.

The rest of this paper is devoted to numerical solution of the boundary value problem specified by eqs.(2), (3) and (5) in the general case  $\theta \neq 0$ , and investigation of the behaviour of the function  $F(\epsilon, \nu)$  at  $\epsilon \gtrsim 1$ . For simplicity reasons we concentrate on particle-induced false vacuum decay in the theory with one scalar field.

## 2 The Model

The choice of particular model turns out to be strongly constrained for technical reasons. After several attempts we ended up with four-dimensional  $-\lambda\phi^4$  theory with the mass term. The action of this model reads

$$S = \int d^4x \left( \frac{1}{2} \partial_\mu \phi \partial^\mu \phi - \frac{1}{2} m^2 \phi^2 + \frac{1}{4} \lambda \phi^4 \right), \quad (9)$$

where  $\lambda$  is a positive constant. At non-zero  $m$  the region  $\phi \approx 0$  and the instability region  $\phi > m/\sqrt{\lambda}$  are separated by a finite energy barrier, and one can ask whether the presence of colliding particles enhances the probability of the barrier penetration (i.e., the decay of the metastable state  $\phi = 0$ ).

It is a lucky coincidence that this model is of special interest for another reason, as it has many features reminiscent of bosonic sector of the Electroweak Theory. At  $m = 0$  (zero Higgs vacuum expectation value) both models are conformally invariant and possess instanton solutions. In the case of  $-\lambda\phi^4$  model the instanton [9] has the action

$$S_{inst} = \frac{8\pi^2}{3\lambda} \quad (10)$$

and describes the decay of the metastable state  $\phi = 0$ . At  $m \neq 0$  (non-zero Higgs vacuum expectation value) the conformal symmetry is softly broken and instanton solutions disappear, while the low energy transitions are described by constrained instantons [10]. The action (10) gets small energy-dependent correction and still determines the transition probability. Like the Electroweak Theory, the  $-\lambda\phi^4$  model possesses the sphaleron solution. The energy of the sphaleron can be found numerically,

$$E_{sph} = 18.9 \frac{m}{\lambda}. \quad (11)$$

Before discussing the discrete formulation of the boundary value problem specified above, it is convenient to rewrite the action (9) in the dimensionless variables. Since the problem is  $O(3)$ -symmetric, we restrict ourselves to  $s$ -wave scattering. The change of variables

$$\phi = \frac{1}{|\mathbf{x}| \sqrt{\lambda}} \psi,$$

$$x = m^{-1}y,$$

brings the action for spherically symmetric configurations to the form

$$S = \frac{4\pi}{\lambda} \int dt \int_0^\infty dr \left[ \frac{1}{2}(\partial_t \psi)^2 - \frac{1}{2}(\partial_r \psi)^2 - \frac{1}{2}\psi^2 + \frac{1}{4r^2}\psi^4 \right], \quad (12)$$

where  $r = |\mathbf{y}|$  is the dimensionless radial distance. Throughout the rest of this paper all dimensionfull quantities are measured in the units of mass.

The starting point for our calculations is the discretized version of the action (12). The system is put on a grid of the size  $L$  with  $n_x + 1$  sites  $r_j = jL/n_x$ ,  $j = 0 \dots n_x$ . Similarly, the time contour is represented by the set of complex points  $t_i$  with  $i = 0 \dots n_t$ . The field  $\psi(t, r)$  transforms into the set of complex variables  $\psi_{ij}$ . To define integrations, we introduce two sets of intervals for each coordinate,

$$\begin{aligned} dr_j &= r_{j+1} - r_j, \quad j = 0 \dots n_x - 1, \\ \tilde{dr}_j &= (dr_{j-1} + dr_j)/2, \quad j = 1 \dots n_x - 1, \\ \tilde{dr}_{0,n_x} &= dr_{0,n_x}/2, \end{aligned}$$

and similarly for  $dt_i$  and  $\tilde{dt}_i$  (tilted and non-tilted intervals are used to integrate fields and derivatives, respectively). With these definitions, the discretized action reads

$$S = \frac{4\pi}{\lambda} \sum_{ij} \left[ \frac{1}{2}(\psi_{i+1,j} - \psi_{ij})^2 \frac{\tilde{dr}_j}{dt_i} - \frac{1}{2}(\psi_{i,j+1} - \psi_{ij})^2 \frac{\tilde{dt}_i}{dr_j} - V_{ij} \tilde{dt}_i \tilde{dr}_j \right], \quad (13)$$

where

$$\begin{aligned} V_{ij} &= \frac{1}{2}\psi_{ij}^2 - \frac{1}{4r_j^2}\psi_{ij}^4 \quad \text{at } j \neq 0, \\ V_{i0} &= 0. \end{aligned}$$

Equations of motion can be easily derived from this action by variation with respect to  $\psi_{ij}$ .

We also need the discrete version of the boundary conditions. Let us start with the final boundary conditions. The first equation (3) transforms into

$$\text{Im } \psi_{n_t,j} = 0.$$

The discrete analog of the second equation can be derived from the requirement that the solution, being continued to the real time axis according to the *discretized* equations of motion, stays real. This requirement leads to the equations

$$\text{Im} \frac{\partial S}{\partial \psi_{n_t,j}} = 0.$$

The discrete reformulation of the initial boundary conditions requires somewhat more work. It can be obtained by means of the following trick. Let us make one step back and treat time as continuous variable. Then we would obtain the  $n_x$ -dimensional quantum mechanical system with the action trivially derived from eq.(13). Since it is assumed that the field reaches linear regime in the initial asymptotic region, we can restrict ourselves to the quadratic part of the resulting action and diagonalize it numerically. In this way we obtain the discrete analog of the momentum representation. Given the corresponding eigenvalues and eigenvectors, it is straightforward to perform the decomposition of the field into positive- and negative-frequency parts and impose boundary conditions (5). Eqs.(5) are then translated into conditions imposed on some linear combinations of  $\psi_{0j}$  and  $\psi_{1j}$ . These are the desired initial boundary conditions in the discrete formulation. To save space we do not present the corresponding cumbersome expressions.

It is instructive to note that the above  $n_x$ -dimensional quantum mechanical system itself can be viewed as a model for studying tunneling transitions from the excited states in multidimensional systems. The action (13) can be treated as discretized (in time) version of the action for this quantum mechanical system. In practice this means that particular number of lattice sites in space direction is not crucial for our conclusions, as long as linear regime can be reached at the initial part of the contour.

### 3 Numerical method

To solve the boundary value problem for given values of  $T$  and  $\theta$  we use a multidimensional version of Newton's method. This is a relaxation procedure which takes as input an approximate solution to the non-linear field equations and improves it at each iteration by solving the linearized equations in the background of the current approximation. Iterations are repeated until non-linear equations are satisfied to the desired accuracy. The advantage of this algorithm is that its convergency requires neither positive-definiteness nor even reality of the action. Moreover, the convergency is quadratic, provided that initial approximation is chosen sufficiently close to the solution. In practice, the accuracy of  $10^{-10}$  is reached in 3–6 iterations.

A drawback of the Newton's method is that its basin of convergency can be very narrow. Thus, it is important to have a good initial approximation at least for some values of  $T$  and  $\theta$ . Then one can move gradually in the  $T - \theta$  plane using output of each run as input for the next one. In our case the starting configuration is provided by the periodic instanton which, at  $E \approx E_{sph}$ , can be approximated by sphaleron plus harmonic oscillation in the sphaleron negative mode (both the sphaleron and its negative mode have to be found numerically). The period of the periodic instanton at  $E \rightarrow E_{sph}$  is determined by the sphaleron negative eigenvalue and equals

$$T_{crit} = 0.78 .$$

The amplitude of the oscillation goes to zero when  $T \rightarrow T_{crit}$ . So, we take  $T \approx T_{crit}$ ,

$\theta = 0$ , and adjust the amplitude of the oscillation in order to get inside the basin of convergency of the periodic instanton with the period  $T$ . In this way we obtain the very first solution to our boundary value problem. Changing  $T$  by small steps we then reproduce the whole family of periodic instantons with different periods. Calculations show that in the  $-\lambda\phi^4$  model the period of the periodic instanton varies from  $T_{crit}$  to zero when the energy decreases from  $E_{sph}$  to zero. This unusual behaviour of period with energy is much in common with that in the  $O(3)$  sigma model [8], where it is also related to softly broken conformal invariance. On the basis of this similarity one should expect the analogous behaviour in the Electroweak Theory.

The Newton's method reduces the non-linear boundary value problem to sequential solution of a few *linear* boundary value problems. At each iteration, to find the correction  $\delta\psi$  to the current approximation amounts to one matrix inversion,

$$\delta\psi = D^{-1}R,$$

where  $D$  is a matrix of second derivatives of the action and  $R$  is a vector of first derivatives, both evaluated at the background. The matrix  $D$  has the dimension  $(2n_t n_x) \times (2n_t n_x)$ , the factor 2 being due to the complexity of the field. In general, the computer time necessary for inversion of such a matrix scales like  $(n_t n_x)^3$ . One can use, however, the fact that this matrix originates from the local second order differential equation and thus is sparse. The sparseness enables one to invert this matrix in  $\propto n_t n_x^3$  operations. Note that for systems containing  $n_f$  fields instead of one, this number would be  $n_t(n_f n_x)^3$ . In practice, to find one solution to the boundary value problem at the grid of dimension  $n_t \times n_x = 200 \times 40$  takes about 5 minutes at SPARCstation 20, most of this time being spent for matrix inversion. The necessary amount of memory scales like  $n_t n_x^2$  and for the above grid is of order 10 Mb.

Let us now discuss constraints on other grid parameters. The most restrictive requirement is that the field must reach linear regime in the asymptotic region A. For that the number of independent modes (which equals  $n_x$ ) must be large enough, and the length of Minkowskian part of the contour,  $T_M$ , must be sufficient to let the energy spread over these modes. Since in the Minkowskian region the most of the field propagates along the light cone, the space size  $L$  should be larger than  $T_M$  to avoid boundary effects. On the other hand, the lattice spacing in  $r$  direction,  $\Delta r$ , should be small enough not only to be close to the continuum limit, but also because otherwise the free spectrum would be cut at too low frequency,  $\omega_{max} \sim \pi/\Delta r$ . This would impose constraints on the available region in the  $E$ - $N$  space,  $E/N \ll \omega_{max}$ , and would not allow for the initial states consisting of small number of high energy particles. Thus, all these arguments push towards large  $n_x$ , which is however bound at relatively low value  $n_x \sim 50 - 100$  by the abilities of available computers.

The number of time slices  $n_t$  is not so constrained since the required computer resources scale linearly with  $n_t$ . In our calculations we take  $n_t$  few times larger than  $n_x$  in order to saturate the continuum limit in time. This number is different for different  $T$  and  $\theta$ .

The particular choice of parameters is model-dependent and is made by trial and error. In the model we consider here rather small value  $T_M = 3$  is sufficient to reach linear regime starting from the vicinity of the sphaleron configuration. Fast linearization is the advantage of high-dimensional models [11] and is due to the volume factor (note  $1/r^2$  in the interaction term in eq.(12)). This effect is absent in two-dimensional models. Moreover, in  $-\lambda\phi^4$  model, the value  $T_M = 3$  is sufficient for linearization at least up to energies  $E \sim 3E_{sph}$ . This feature differs the above model from other four-dimensional models we have tried.

Fast linearization allows to take relatively small space size,  $L = 3$ , which leads to the sufficiently wide spectrum already at  $n_x = 40$ . The free spectrum for these values of parameters reproduces the continuum spectrum with reasonable accuracy up to  $\omega \sim 15$ .

## 4 Results and discussion

The results presented in this this paper were obtained at  $L = 3$ ,  $T_M = 3$ ,  $n_x = 40$  and  $n_t$  varying from 200 to 300. For these values of grid parameters we have found about 1500 solutions to the boundary value problem with different  $E$  and  $N$ . The region of  $\epsilon$ - $\nu$  plane covered by the solutions is shown in Fig.2. The top left corner of the solution region (point S in Fig.2) is the sphaleron. It corresponds to  $\epsilon = \nu = 1$ . At this point the function  $F(\epsilon, \nu)$  vanishes and exponential suppression of probability disappears.

Towards small energies the solution region is bound by the line of periodic instantons (the line SP in Fig.2). In the continuum limit this line would end up at the point  $\epsilon = \nu = 0$  which corresponds to the zero energy instanton. However, the spatial size of periodic instantons rapidly decreases along this line. At the above values of grid parameters, the instanton size becomes comparable to the lattice spacing at  $\epsilon \approx 0.4$  (the point P in Fig.2). At this point the Newton's algorithm stops to converge. Along the line of periodic instantons, the function  $F(\epsilon, \nu)$  monotonically decreases and reaches the value  $F = -0.6S_{inst}$  at the point P.

The boundary of convergency continues at approximately constant  $\nu$  towards higher energy. It is represented by the line PQ in Fig.2. The function  $F$  is negative along this line.

The third boundary of the solution region is formed by the line  $F = 0$  (solid line in Fig.2). It starts at the sphaleron and goes towards higher energy and smaller number of particles. At energy  $E \approx 3E_{sph}$  it comes close to the boundary of convergency, which makes finite the available part of  $\epsilon$ - $\nu$  plane. Our data cover this available region.

In this paper we concentrate on the dependence of the function  $F$  on energy and number of particles. It is most conveniently represented by the lines of constant  $F$  in the  $\epsilon$ - $\nu$  plane. These lines can be obtained by interpolation and are shown in Fig.3. They start at the line of periodic instantons with infinite negative slope. The latter

can be seen analytically. Indeed, from eqs.(6) and (8) one immediately derives that

$$\frac{\partial N}{\partial E} \Big|_F = -\frac{2T}{\theta}. \quad (14)$$

The slope  $\partial N/\partial E|_F$  becomes infinite at the periodic instantons where  $\theta = 0$ .

The function  $F(\epsilon, \nu)$  determines the maximum probability of induced false vacuum decay among  $N$ -particle initial states. The line  $F = 0$  separates the classically forbidden and classically allowed regions. We see from Fig.3 that for each energy  $E > E_{sph}$  there exists a minimum number of particles  $N_{crit}(E)$  for which the decay may occur classically without exponential suppression. At  $N > N_{crit}$  one thus may expect the existence of classical configurations which pass above the barrier. On the other hand, at  $N < N_{crit}$  all classical solutions bounce off the barrier. By continuity, when  $N$  approaches  $N_{crit}$  from above, the classical solutions which pass above the barrier should spend more and more time on its top oscillating above the sphaleron, so that in the limit  $N = N_{crit}$  this time goes to infinity.

At  $N < N_{crit}$ , the decay is a tunneling event which is described by corresponding solution to our boundary value problem. As discussed above, the real time part of this tunneling solution represents the classical evolution of the system after barrier penetration. In our model this evolution leads to the singularity (point P in Fig.1). In between two singularities on the real time axis, the tunneling solution represents the field which comes from infinity, bounces off the barrier and goes back to infinity. When  $N$  approaches  $N_{crit}$  from below, the distance between two singularities grows (see Fig.4) and the solution spends more and more time around the sphaleron. Although due to instabilities we were not able to trace the positions of singularities when the distance between them becomes of order one, we expect that at the line  $F = 0$  this distance goes to infinity and the real time part of the tunneling solution reproduces the infinitely oscillating classical solution described above. Thus, the configurations which correspond to the line  $F = 0$  should be classical solutions infinitely oscillating above the sphaleron.

Due to the existence of minimum number of particles at fixed energy  $E$ , one can try to obtain the line  $F = 0$  by minimizing  $N$  over the set of classical solutions which pass above the barrier. This strategy was used in ref.[11] to set bounds on the forbidden region. We have tried to use this strategy to reproduce the line  $F = 0$  found by the tunneling approach. We have obtained bounds which are noticeably higher than the real position of this line. The reason could be that the classical solutions which correspond to the line  $F = 0$  are infinitely oscillating around the sphaleron and thus are singular points of the space of solutions which pass above the barrier.

As one can see from Fig.3, the size of allowed region increases towards higher energy, while the minimum number of particles for which the decay is not exponentially suppressed, decreases. We have traced this behaviour up to  $E \sim 3E_{sph}$  where the absence of convergency prevents us from going further with the same grid parameters. Since the probability  $\sigma(E, N)$  is an upper bound for the two-particle cross section at

energy  $E$ , we conclude that the latter cross section is exponentially suppressed at  $E < 3E_{sph}$ . Moreover, extrapolating the behaviour of  $N_{crit}(E)$  and assuming that the derivative  $\partial N_{crit}(E)/\partial E$  continues to decrease in absolute value, one can see that the line  $F = 0$  does not cross the  $N = 0$  axis at least up to  $E \sim 10E_{sph}$ . Thus, we conclude that exponential suppression of the two-particle cross section persists at least up to  $E \sim 10E_{sph}$ .

Careful look at the data shows that the behaviour of the function  $F(\epsilon, \nu)$  may qualitatively change at substantially lower energy. To see this consider the slope of the lines of constant  $F$  as a function of  $E$ . The derivative  $\partial N/\partial E|_F$  can be expressed through the known parameters according to eq.(14). Its behaviour with energy is shown in Fig.5. Extrapolating, one can see that it would become zero at  $E_* \approx 3.5E_{sph}$  and  $N_* \approx 0.35N_{sph}$ . If this indeed happens, then starting at this energy the line  $F = 0$  in coordinates  $E$  and  $N$  would turn up ( $dN_{crit}(E)/dE$  would become positive), while the function  $F(E, N_*)$  at  $E > E_*$  would decrease with energy. Clearly, this behaviour is unphysical. Indeed, it is always possible to put the excess energy  $E - E_*$  in one quantum particle and thus effectively decrease the energy involved in the semiclassical tunneling, leaving the number of particles practically unchanged. The corresponding initial state would not be semiclassical, and its probability of tunneling would be  $F(E_*, N_*)$ , i.e. higher than follows from the semiclassical picture. If this situation realizes, it is natural to expect that starting at  $E = E_*$  the correct function  $F(E, N_*)$  stays constant and thus the line  $F = 0$  never crosses the  $N = 0$  axis. The latter would mean that the two-particle cross section is always exponentially suppressed.

As is clear from Fig.3, in order to go to higher energies and verify the above conclusions based on extrapolation, one has to extend the convergency region towards smaller number of particles. The breakdown of convergency is most likely related to the lattice spacing in  $r$  direction. We have checked that doubling  $n_x$  at fixed  $L$  extends the convergency region for periodic instanton solutions. We expect that the same effect persists at  $\theta \neq 0$ . Thus, increasing  $n_x$  could be the way to extend the convergency region and improve our results. This, however, will require noticeably more computer resources.

In conclusion, we would like to stress again the analogy, as long as instanton-like transitions are concerned, between the  $-\lambda\phi^4$  model and the bosonic sector of the Electroweak Theory. On the basis of this analogy, we expect that the Electroweak Theory is also a suitable model for studying instanton-like transitions numerically. Since, because of larger number of fields, calculations there are at least  $4^3$  times slower, they would require the use of computers much faster than a typical workstation.

## Acknowledgments

The authors would like to thank V.A.Rubakov and D.T.Son for numerous and fruitful discussions at different stages of this work. The work is supported by ISF grant #MKT300 and INTAS grant #INTAS-94-2352. The work of P.T. is supported in

part by Russian Foundation for Fundamental Research, grant #93-02-3812.

## References

- [1] A.Ringwald, *Nucl.Phys.* **B330** (1990) 1,  
O.Espinosa, *Nucl.Phys.* **B334** (1990) 310.
- [2] M.Mattis, *Phys.Rep.* **214** (1992) 159,  
P.G.Tinyakov, *Int.J.Mod.Phys.* **A8** (1993) 1823.
- [3] V.A.Rubakov and P.G.Tinyakov, *Phys.Lett.* **B279** (1992) 165.
- [4] P.G.Tinyakov, *Phys.Lett.* **B284** (1992) 410.
- [5] V.A.Rubakov, D.T.Son and P.G.Tinyakov, *Phys.Lett.* **287B** (1992) 342.
- [6] S.Yu.Khlebnikov, V.A.Rubakov and P.G.Tinyakov, *Nucl.Phys.* **B367** (1991) 334.
- [7] V.V.Matveev, *Phys.Lett.* **B304** (1993) 291.
- [8] S.Habib, E.Mottola and P.G.Tinyakov, preprint CERN-TH-7432-94, 1994, hep-ph/9411251.
- [9] S.Fubini, *Nuovo Cimento* **A34** (1976) 521,  
L.N.Lipatov, *Zh. Eksp. Teor. Fiz.* **72** (1977) 411.
- [10] I.Affleck, *Nucl.Phys.* **B191** (1981) 455.
- [11] C.Rebbi and R.Singleton, preprint hep-ph/9502370, Boston University (1995).

## Figure captions

**Fig.1.** The contour ABCD in the complex time plane where the boundary value problem is formulated. Crossed circles represent singularities of the field. Dotted line schematically shows the deformed contour used in numerical calculations.

**Fig.2.** The  $\epsilon$ - $\nu$  map of the obtained solutions. The point S corresponds to the sphaleron. Crossed circles lying on the line SP are periodic instantons. The line PQ represents the boundary of convergency region, while the solid line corresponds to  $F(\epsilon, \nu) = 0$ .

**Fig.3.** The lines of constant  $F(\epsilon, \nu)$  in the  $\epsilon$ - $\nu$  plane. Numbers show the value of  $F$  in the units of  $S_{inst}$ .

**Fig.4.** The distance between singularities  $\Delta t$  as a function of  $F$  when  $F$  approaches zero. Dashed line corresponds to the region where the procedure of calculating  $\Delta t$  is not reliable.

**Fig.5.** The dependence of  $-\partial N/\partial E|_F = 2T/\theta$  on  $\epsilon$ . Dashed line represents the extrapolation to higher energies.  $\epsilon_* = E_*/E_{sph}$  corresponds to the point where the behaviour of  $F(\epsilon, \nu)$  may qualitatively change.

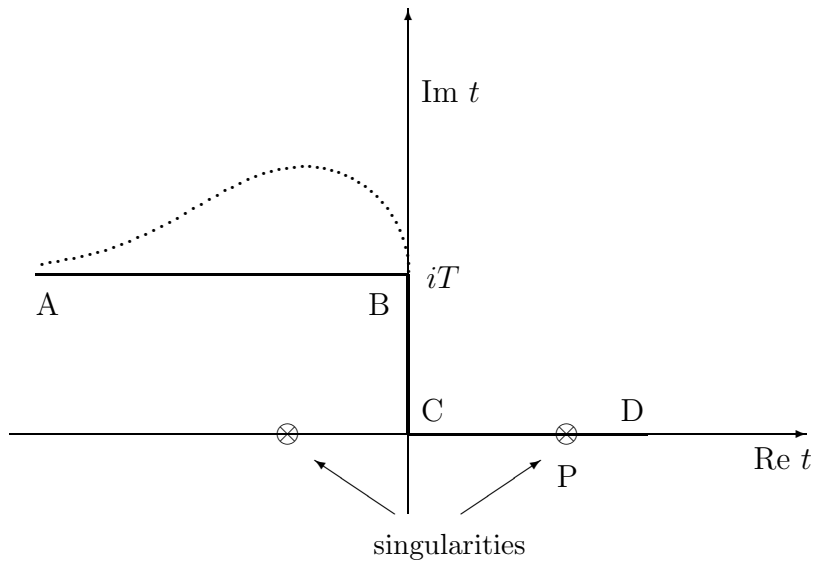


Fig.1

Fig.2

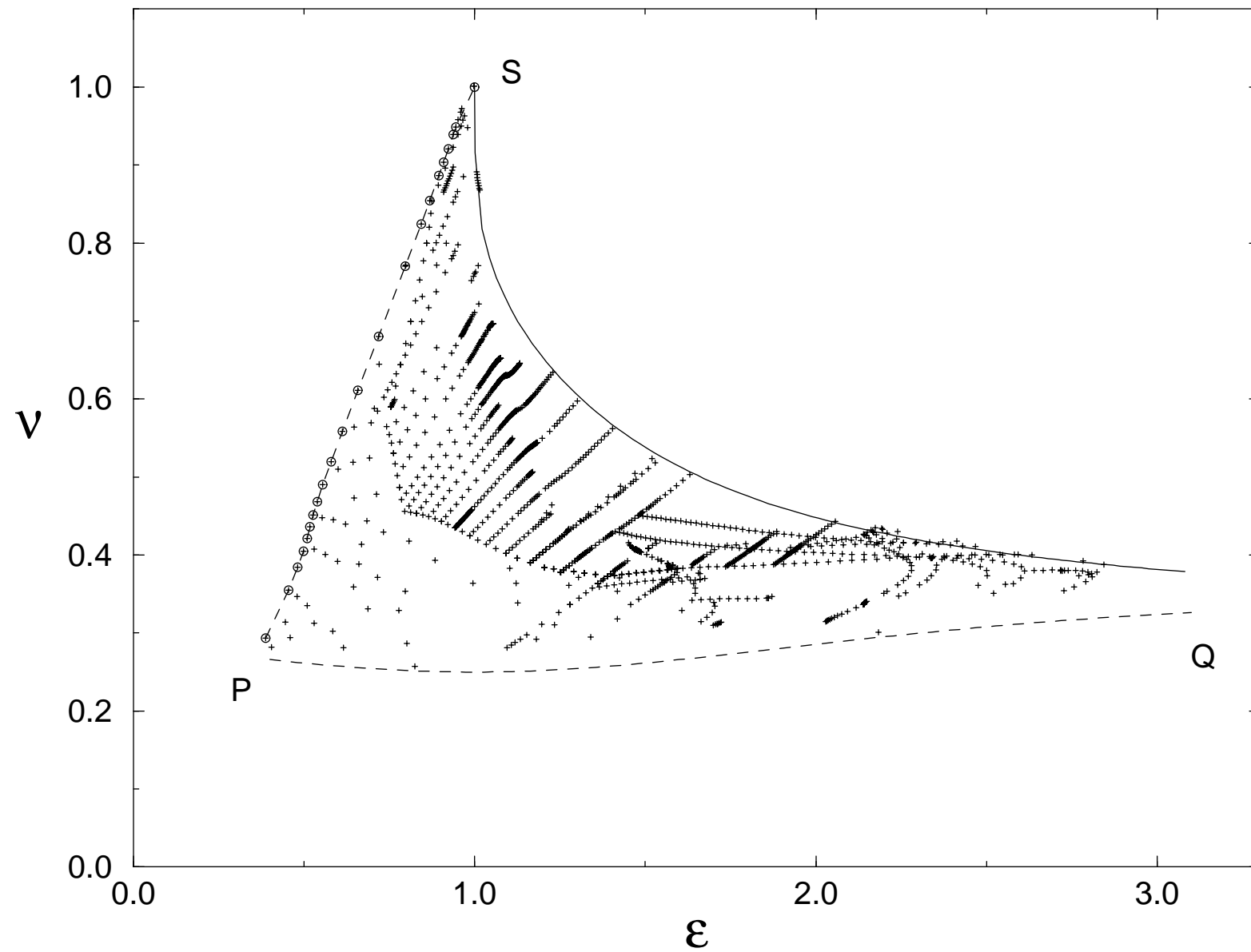


Fig.3

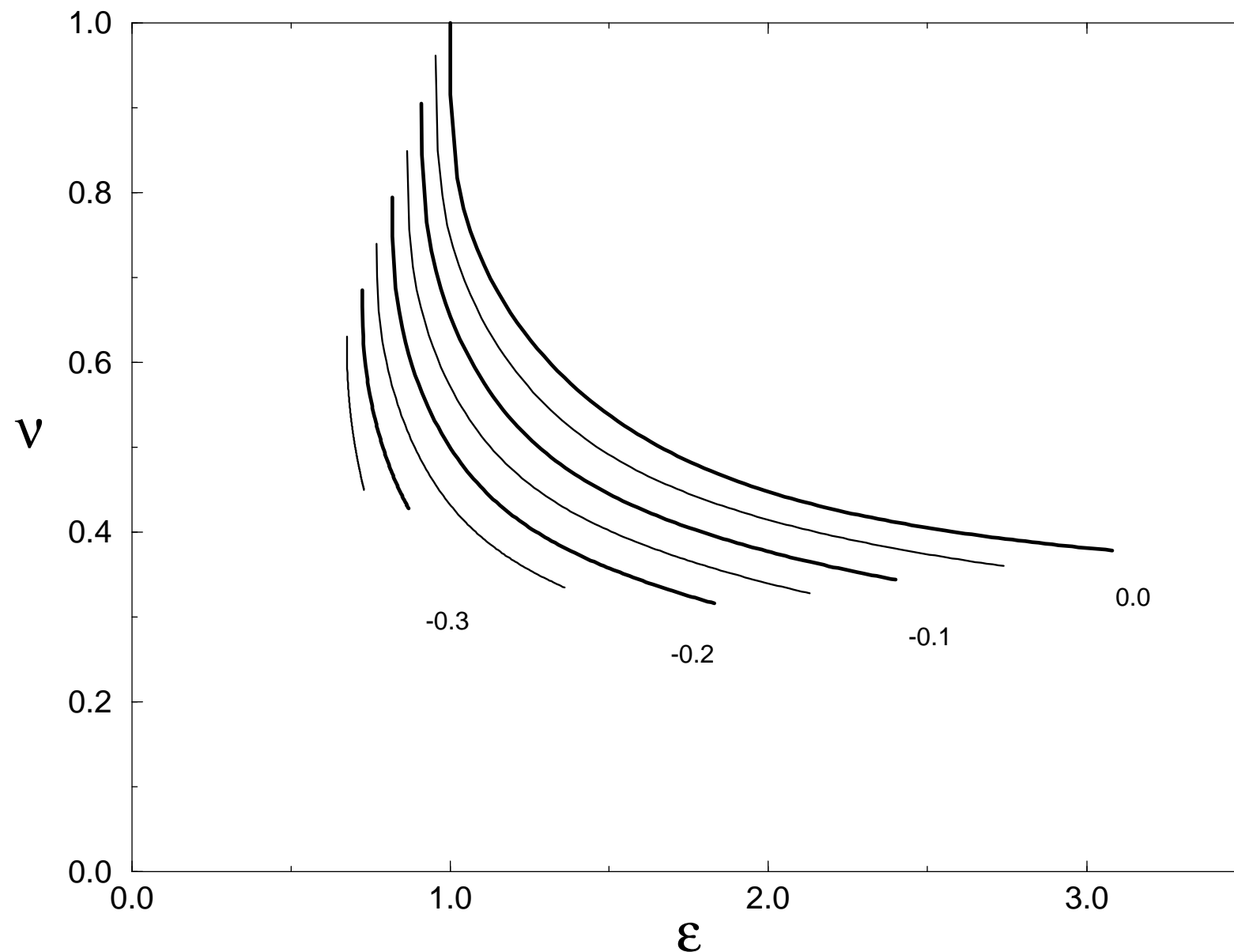


Fig.4

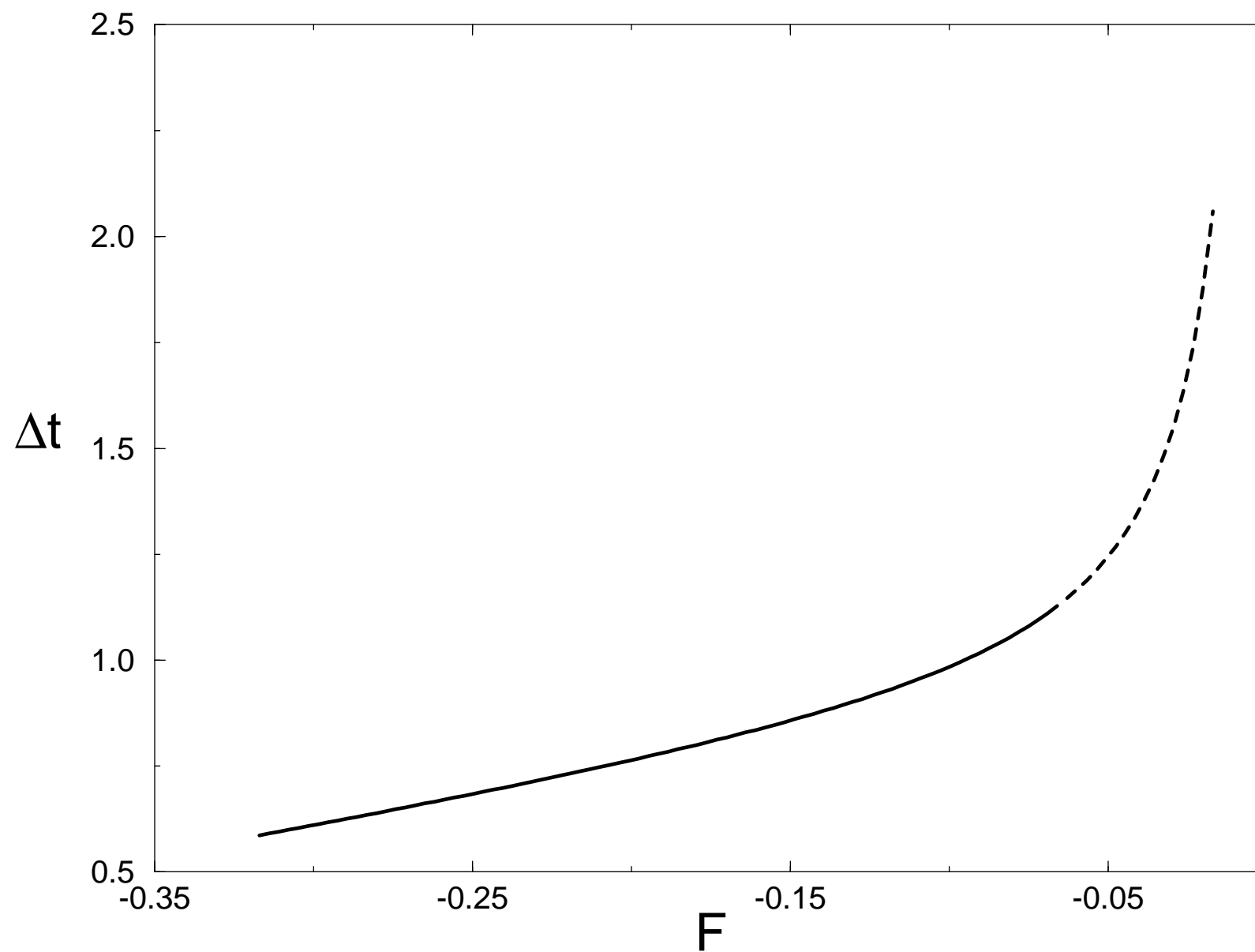


Fig.5

